A theoretical study of the melting curve of iron to very high pressure

1989 J. Phys.: Condens. Matter 1 5243

(http://iopscience.iop.org/0953-8984/1/31/023)

J. Phys.: Condens. Matter **1** (1989) 5243–5252. Printed in the UK

A theoretical study of the melting curve of iron to very high pressure

C Hausleitner and J Hafner
Institut für Theoretische Physik, Technische Universität Wien, Karlsplatz 13, A 1040 Wien, Austria

Received 30 November 1988

Abstract. We present a detailed theoretical study of the melting curve of iron from normal conditions up to pressures of 1.5 Mbar, i.e. up to pressures characteristic for the boundary between the Earth's mantle and its core. The analysis is based on simple effective inter-atomic pair interactions derived from a combined nearly free-electron treatment of the s electrons and a tight-binding treatment of the d electrons. The free energies of the solid and liquid phase are calculated using thermodynamic variational methods. For the solid we use an Einstein reference system. For the liquid both hard-sphere and soft-sphere variational systems are investigated. The soft-sphere reference system produces a lower (and hence more accurate) liquid free energy. This is necessary to achieve a quantitative description of the melting properties. In particular, the predicted increase of the melting temperature with pressure is in reasonable agreement with recent measurements reported by Q Williams and co-workers.

1. Introduction

Iron is considered to be the dominant constituent of the Earth's core; thus the variation of the melting temperature of iron with very high pressures is of considerable theoretical and experimental interest [1–3].

The calculation of the melting curve of a metal from first principles remains a challenging problem—the latent heat of fusion being only a very small fraction of the cohesive energy [4]. For simple metals, the foundations of a quantitative theory of melting were laid some time ago by Ashcroft and Stroud [5] and Jones [6]. The basic ingredients of the approach are pseudopotential perturbation theory for the construction of effective inter-atomic pair interactions, and various thermodynamic perturbation theories for calculating the free energies of the solid and liquid phases. On this basis a reasonably quantitative description of the melting properties has been achieved for the alkali metals [5–8], for Al [9, 10], Sr [11] and Pb [12]. Other attempts to study the solid/liquid transition in s–p-bonded metals or semiconductors are based on either molecular dynamics [13–15] or density functional theory [16].

For the more interesting case of the transition metals progress has been rather slow. This is mainly due to the lack of reliable inter-atomic potentials. Recently Wills and Harrison [17] have extended the nearly free-electron theory of simple metals to include the effects of the transition-metal d bands. This is achieved by using a simplified tight-binding description and a momentum decomposition of the d-electron density of states

0953-8984/89/315243 + 10 $02.50

and results in a bonding pair interaction proportional to the width of the d band and a repulsive interaction arising from the shift of the centre of gravity of the d band. These pair interactions add to the simple-metal-like pair potential mediated by the s electrons, the total pair potential being much stronger than in simple metals. Using a slightly modified form of the Wills–Harrison potentials and a thermodynamic variational technique with a soft-sphere reference medium we have recently succeeded in describing the structure and the thermodynamic properties of the liquid 3d and 4d transition metals with reasonable accuracy [18].

In the present paper we combine the variational description of the liquid free energy with a variational calculation of the free energy of the solid based on an Einstein reference system. In § 2 we summarise the elements of the simplified approach to the cohesive and structural properties of transition metals. In § 3 we review the statistical mechanical calculation of the free energies. Then in § 4 we present and discuss the results for the melting of iron.

2. Effective pair interactions for transition metals

Following Wills and Harrison [17] the nearly free-electron theory for simple metals is extended to include the effect of the transition-metal d bands by using the Friedel model of the d-electron density of states and an atomic sphere approximation for the d–d transfer and overlap integrals. This produces a bonding term proportional to the d-band width and a repulsive term arising from the shift of the centre of gravity of the d band. The effect of the s–d hybridisation is included through a variation of the relative occupancies of the s and d bands. By writing the bond energies in terms of the moments of the d–d interactions, we may express them in terms of effective pair interactions. Altogether the total energy is composed of a volume term $E_0(\Omega)$, and a sum over density-dependent pair interactions. The pair potential consists of an s-electron contribution $V_s(r)$ and a d-electron contribution $V_d(r)$,

$$V(r) = V_s(r) + V_d(r). \tag{1}$$

The s-electron contribution is given in terms of the electron–ion pseudopotential (we assume an empty-core model with a core radius R_c) and the dielectric response functions $\chi(q)$ and $\varepsilon(q)$ are given by the familiar expressions ([4], pp 69ff)

$$V_s = 2Z_s^2 \left(1 + 16 \int_0^\infty (\chi(q)/\varepsilon(q)) \cos^2(qR_c) \sin(qr)/q^3 \, dq\right) \Big/ r \tag{2}$$

where Z_s is the number of s electrons (we use $Z_s = 1.5$ for all transition metals, in accordance with [17] and the result of self-consistent band-structure calculations—see, e.g., [19]). The d-electron contributions are given by [17, 18]

$$V_d = -[Z_d(10 - Z_d)/10(28.06/\pi)]2R_d^3/r^5 + Z_d(450/\pi^2)R_d^6/r^8 \tag{3}$$

where Z_d is the number of d electrons and R_d is the d-state radius. Z_d is fixed by setting $Z_s = 1.5$. For R_d we use the d-state radii determined by Harrison and Froyen [20] by fitting the width of the canonical bands calculated in the atomic sphere approximation.

This leaves us with the empty-core radius as the single free parameter in the theory. We determined R_c by fitting the density of crystalline iron at room temperature. This yields $R_c = 1.703$ au (in [18] we used a somewhat different core radius derived from a simplified equilibrium condition).

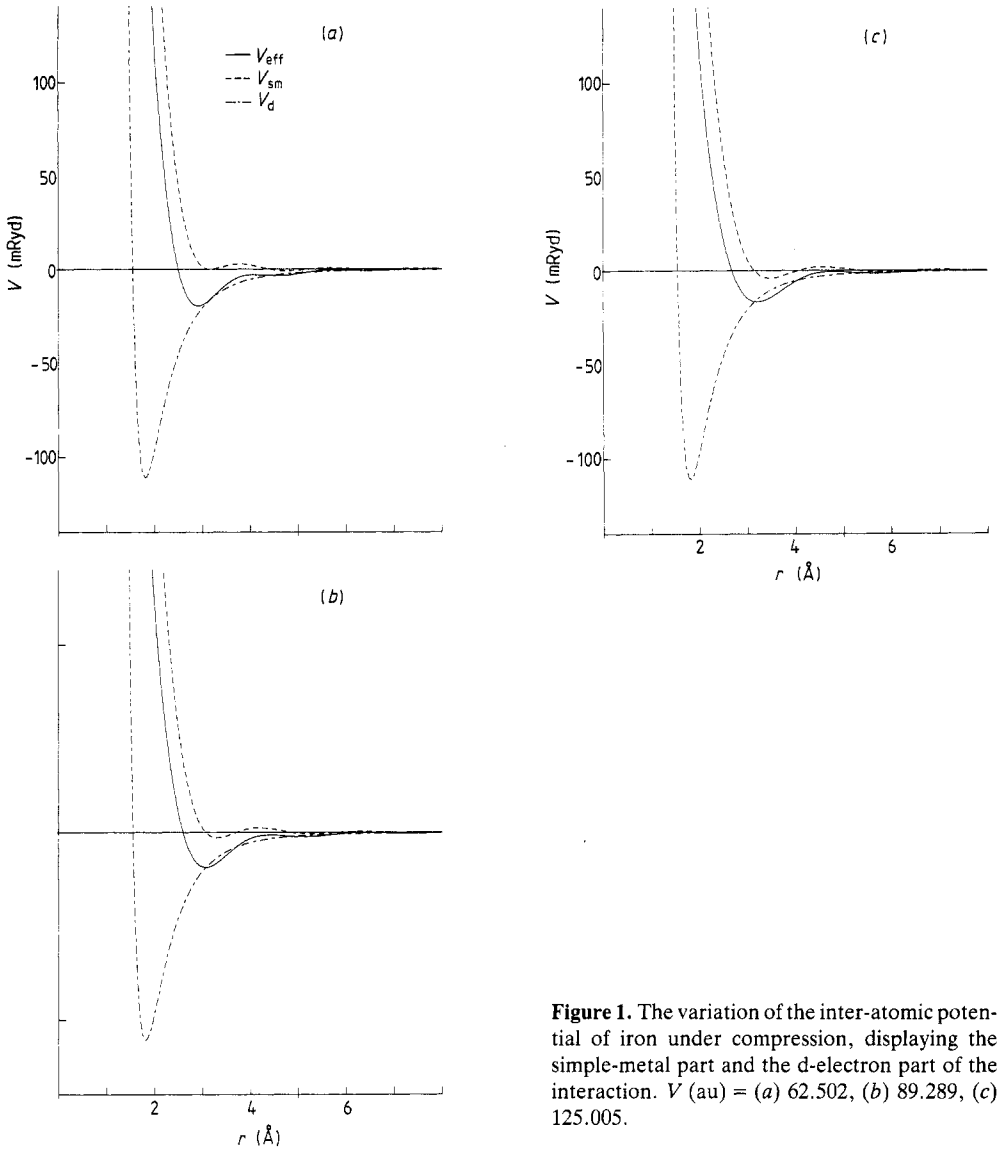

Figure 1. The variation of the inter-atomic potential of iron under compression, displaying the simple-metal part and the d-electron part of the interaction. V (au) = (*a*) 62.502, (*b*) 89.289, (*c*) 125.005.

Figure 1 shows the effective inter-atomic potentials as functions of volume. Only the s-electron contribution varies with the electron density. The d-electron part behaves like a classical pair potential. The net effect on the inter-atomic interaction is to shift the minimum to smaller distances under compression.

3. Statistical mechanics

According to the Gibbs–Bogoliubov inequality [21] an upper bound to the exact free energy is given by

$$F \leqslant U_0 + E_{fe} + \langle E_{es} \rangle_0 + \langle E_{bs} \rangle_0 + \langle E_d \rangle_0 - T(S_0 + S_{el}) \tag{4}$$

where U_0 is the kinetic energy of the ions in the reference system, E_{fe} is the free-electron

energy, the third to fifth terms are the electrostatic, band-structure (s-electron), and d-electron energies, averaged over the ionic coordinates, and S_0 and S_{el} are the reference system entropy and the electronic entropy, respectively. For the electronic contribution to the entropy we use, in accordance with our electronic structure model,

$$S_{el} = \gamma Z_s T + (\pi^2/3)k_B^2 n_d(E_F)T \tag{5}$$

where γ is the Sommerfeld constant of the electronic specific heat and the d-electron density of states $n_d(E)$ is calculated from the Friedel model.

3.1. Solid phase

For the solid phases we have chosen for simplicity an Einstein model as a reference system. The kinetic energy and the entropy term are given by [4, 22]

$$U_0 - TS_0 = 3k_B\theta_E[\tfrac{1}{4}\coth(x/2) + (\exp(x)-1)^{-1} - \ln(1-\exp(-x))/x] \tag{6}$$

with $x = \theta_E/T$ where θ_E is the Einstein temperature. The structure-dependent terms in (4) are given by the usual expressions, with each phase factor $\exp(-i\boldsymbol{q}\cdot\boldsymbol{R}_l)$ entering the structure factor replaced by its thermal expectation value evaluated in the Einstein reference system:

$$\langle\exp(i\boldsymbol{q}\cdot\boldsymbol{R}_l)\rangle_0 = \exp(i\boldsymbol{q}\cdot\boldsymbol{R}_{l0})\exp(-q^2\mu). \tag{7}$$

The mean square amplitudes of vibration are given by

$$\mu = \coth(\theta_E/2T)/4Mk_B\theta_E. \tag{8}$$

The upper bound to the free energy is obtained by minimising the right-hand side of (4) with respect to θ_E. Note that the variational approach is, within the bounds of the reference system, equivalent to a self-consistent phonon approximation, i.e. even-order anharmonicities are included to all orders.

3.2. Liquid phase

For the liquid phase we have shown that a hard-sphere Yukawa (HSY) fluid is a very appropriate reference system for materials with hard- or soft-core interactions. Analytical solutions for the structure factor are available in the mean-spherical approximation [4, 18, 23]. The variational upper bound to the liquid free energy is given by an expression analogous to (4). It has to be minimised with respect to three parameters: the diameter σ of the hard core (or equivalently the hard-sphere packing fraction $\eta = \pi\sigma^3/6\Omega_a$ where Ω_a is the atomic volume), the strength ε of the Yukawa potential at hard contact, and the inverse screening length κ (for details, see [4, 18]). Note that for all liquid transition metals the HSY reference fluid yields a lower variational free energy than a simple hard-sphere reference liquid [18].

4. Melting curve

The melting curve is established by the common-tangent construction on the free energy versus volume curves of the solid and liquid phases at a fixed temperature $T = T_m$. This yields directly the melting pressure $p_m(T_m)$.

In the case of iron the calculation of the melting curve is complicated by two facts. (i) iron undergoes a polymorphic transition from the FCC γ-phase to the BCC δ-phase at a temperature $T_{\gamma\delta} = 1665$ K not too far below the melting temperature $T_m = 1809$ K [2]. The γ–δ transition curve intersects the melting curve of δ-iron at a γ–δ–L triple point close to $p = 50$ kbar and $T = 2000$ K. At pressure above 50 kbar the melting of the γ-phase is observed. (ii) The low-temperature polymorphic transitions from the BCC α-phase to the γ-phase ($T_{\alpha\gamma} = 1184$ K) and the pressure-induced transition from the ferromagnetic α-iron to the non-magnetic HCP ε-phase ($p \simeq 170$ kbar) are dominated by magnetic effects. The polymorphic transitions have been discussed frequently in the literature [24–26]. The ferromagnetic energy contribution stabilises the BCC phase with respect to the close-packed structures at $T = 0$ K. At higher temperatures the α-phase is destabilised by the rapid increase of the magnetic entropy as the ferromagnetically aligned moments become disordered. It has been shown that disordered local moments can be sustained within a band framework above the Curie tempeature T_C and also in the paramagnetic and non-magnetic phases [25–26]. The root mean square local magnetic moments increase strongly upon volume expansion. At temperatures above T_C they are nearly the same in all three crystalline phases. Thus it appears to be legitimate to assume that the liquid phase shows the same degree of spin disorder as the crystalline phases. This would explain why the entropy of melting of δ-iron ($S = 0.92\ k_B$) comes very close to the normal value for all BCC metals ($S = (0.91 \pm 0.17)\ k_B$) [24, 27]. As the liquid has a large atomic volume, it would also be in line with the increase of the magnetic moments under expansion.

Hence the assumption that the melting of iron is not influenced by the magnetic effects seems to be an acceptable working hypothesis. On the other hand we cannot ignore the fact that close to the melting line we have a competition between two crystallographic phases. This means that we have to calculate the crystalline free energies for both the BCC δ-phase and the FCC γ-phase and determine their melting curves via two independent sets of common-tangent constructions. The intersection of the two melting curves defines the γ–δ–L triple point.

Figure 2 shows the free energy versus volume curves at different temperatures. In (*a*) we compare the BCC phase and the liquid (treated in the HSY reference system). In (*b*) we compare the FCC phase and the liquid. A compilation of calculated zero-pressure thermodynamic data for the solid and liquid phases is given in table 1 and compared with experimental data. We find a reasonable agreement for the calculated densities and entropies, albeit with a general trend towards underestimation of the entropy in the solid as well as in the liquid phases. The result for the solid phases is remarkable in that we find only a minimal difference in the effective Einstein temperatures θ_E and hence in the vibrational free energies of the two competing phases. Thus the γ–δ transition is not associated with vibrational effects. On the other hand we find that the d-electron contribution to the structural energy difference varies strongly with the volume, the close-packed phase being stabilised under compression. For the liquid phase we confirm our previous result [18] that the HSY result gives a significantly lower variational upper bound to the free energy than does the HS system.

The melting curve is determined by the common-tangent construction. As the free energy of the liquid phases increases more rapidly under compression we expect an increase of the melting temperature under compression. The calculated melting properties for γ- and δ-iron are summarised in table 2. Figure 3 shows a comparison of the calculated melting curves for pressures up to 3 Mbar, compared with the recent experimental results of Williams and co-workers [1] from laser-pulse melting experiments in a diamond-anvil cell.

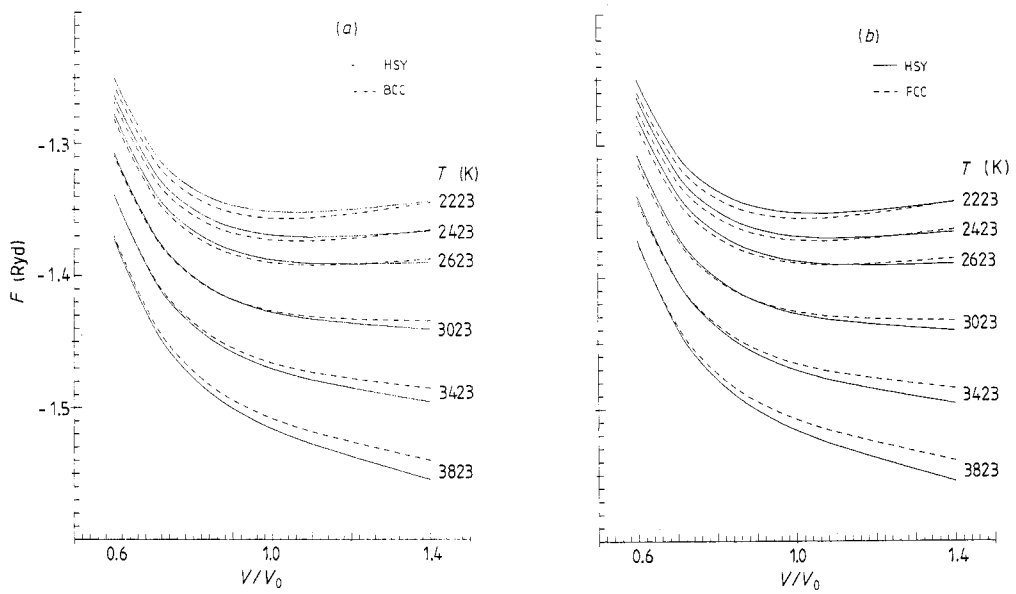

Figure 2. Free-energy curves of the BCC (*a*) and FCC (*b*) phases compared with those of the melt.

Table 1. Calculated thermodynamic properties of iron in the solid and liquid phases: atomic volume Ω_a, entropy S, and variationally determined parameters of the Einstein and HSY reference systems (θ_E, η, ε, κ—see the text).

			Ω_a (Å^3)		S/k_B			
	T (K)	θ_E (K)	Calc.	Exp.[a]	Calc.	Exp.[b]		
γ-iron	1473	345	12.31	12.26	8.52	10.05		
	1673	341	12.46		9.11			
	1873	337	12.65		9.68			
δ-iron	1473	346	12.39		8.52			
	1673	342	12.55	12.35	9.12	10.65		
	1873	337	12.75		9.70			
					Ω_m (Å^3)		S/k_B	
	T (K)	η	ε (mRyd)	κ (au^{-1})	Calc.	Exp.[c]	Calc.	Exp.[b]
Liquid iron	2223	0.431	183	0.90	13.42	13.84	11.80	13.14
	2423	0.415	176	0.93	13.68	14.27	12.48	13.62
	2623	0.402	172	0.94	13.99	14.63	13.12	14.06

[a] After [28].
[b] From [29].
[c] After [30].

Our calculated melting curves show reasonable agreement with experiment. The melting temperature increases quite strongly under pressure. This increase is more pronounced for the FCC than for the BCC phase, the two curves intersect at a γ–δ–L triple

Table 2. Calculated melting properties of γ- and δ-iron: melting temperature T_m, melting pressure p_m, fractional volume change on melting $\Delta\Omega$, entropy of fusion S, and Lindemann ratio L.

	T_m (K)	p_m (kbar)	$\Delta\Omega$ (%)	S/k_B	L
γ-iron (FCC)	2640	0			
	3023	263	1.4	1.28	0.068
	3423	671	1.8	1.17	0.065
	3823	1019	2.2	1.12	0.067
	4223	1581	2.4	2.10	0.069
Exp.[a]	2000	50			
δ-iron (BCC)	2680	0			
	3023	225	0.9	1.30	0.077
	3423	1079	0.7	0.94	0.073
	3823	1813	0.8	0.58	0.074
	4223	2361	1.2	1.49	0.075
Exp.[b]	1809	0	6.2[c]	0.92[d]	
				1.03[e]	

[a] γ–δ–L triple point.
[b] Zero-pressure melting of δ-iron.
[c] After [28].
[d] After [29].
[e] After [31].

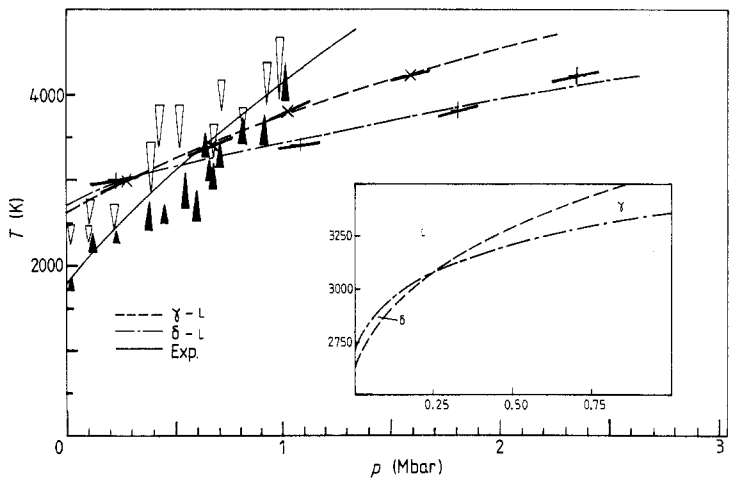

Figure 3. Melting curves of BCC and FCC iron, calculated using the HSY and Einstein reference systems. The crosses give the calculated points, the short bars the slopes of the melting curves calculated from the Clausius–Clapeyron relation $dT_m/dp_m = \Delta\Omega/\Delta S$. The broken (FCC) and chain (BCC) curves are tentative interpolations of the melting curves. The open and full arrow heads show upper and lower estimates to the melting point inferred from the laser-pulse experiments of Williams and co-workers [1]. The full curve is a tentative interpolation of the experimental results. The region around the triple point is shown enlarged in the inset.

point at a pressure of about 200 kbar. The stabilisation of the FCC phase under pressure stems from a lower d-electron energy, the entropy contributions being nearly the same for the two crystalline phases.

Within the HSY reference system for the liquid the largest independent error is a 40% overestimate of the melting temperature, compared with a 13% accuracy achieved in similar calculation for the simple metal Al [10]. The calculated melting temperature depends quite critically on the reference system. If the HSY reference system for the liquid metal is replaced by a HS reference system, then the calculated melting temperature would be even higher, by $\simeq 400$ K. However, if the HSY reference system describes the softness of the transition-metal pair interactions quite well, it does not account for the effect of the attractive interactions on the liquid structure. These attractive interactions are much stronger for transition metals than for simple metals. This explains the relatively modest result for the calculated melting temperature of iron. On the other hand this is also why atempts to apply more sophisticated perturbation methods such as the optimised random-phase approximation to liquid transition metals have up to now been unsuccessful.

Other properties, such as the fractional volume change on melting and the entropy of fusion, are much less sensitive to the choice of reference system and we find a quite reasonable agreement with experiment.

It is well known that the solid/liquid transition obeys two empirical rules: the Lindemann rule on the solid side, and the Verlet rule on the liquid side of the melting curve. According to the former the Lindemann ratio L (the root mean square displacement divided by the nearest-neighbour distance) should be constant along the melting curve [32]. In our calculation we find that L remains very nearly constant over a very wide range of pressures (table 2). Verlet's rule [33, 34] predicts that a melt freezes when the height of the first peak of the static structure factor reaches a value of $S(Q_P) \simeq 2.8$ and that the structure factor as a function of the momentum transfer scaled to Q_P should vary very little along the melting line. Again we find that liquid iron obeys this rule up to very high pressures (see figure 4).

5. Conclusions

We have presented the first calculation of the melting curve of a transition metal starting from an electronic theory of the interaction forces. For the difficult case of iron we find encouraging results. The calculations correctly predict a γ–δ–L triple point, an increase of the melting temperature under pressure in reasonable agreement with recent experiments, and quite acceptable values for the volume and entropy changes on melting. The largest error occurs for the low-pressure melting temperature.

Altogether it is certainly surprising that even semi-quantitative agreement with experiment can be achieved with such an extremely simplified form of the inter-atomic interaction and such a simple reference system, allowing questions of metallurgical and even geophysical significance to be addressed with methods that are essentially rigorous and developed from first principles. Future work will bear on improved inter-atomic potentials, on anharmonic corrections to the vibrational free energy of the crystal and on a better description of the structure and the thermodynamics of the melt.

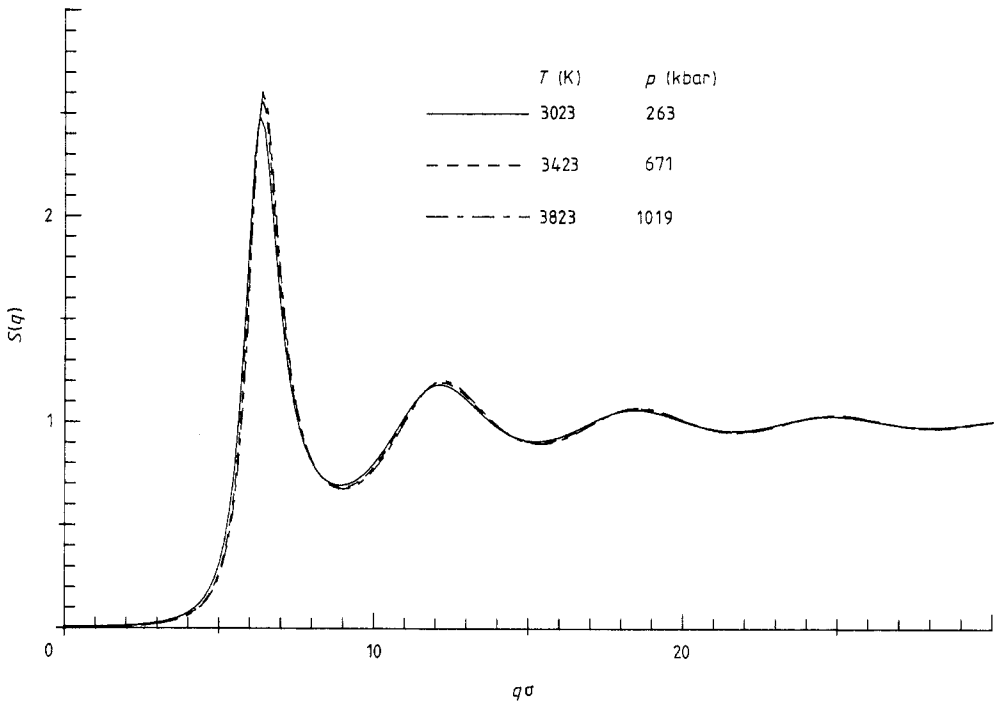

Figure 4. The variation of the static structure factor of liquid iron along the melting curve, plotted as a function of the scaled momentum transfer $q\sigma$ (σ is the variationally determined HSY diameter).

Acknowledgment

This work was supported by the Fonds zur Förderung der wissentschaftlichen Forschung (Austrian Science Foundation) under project No 6191.

References

[1] Williams Q, Jeanloz R, Bass J, Svendsen B and Ahrens T J 1987 *Science* **236** 181
[2] Liu L G and Bassett W A 1975 *J. Geophys. Res.* **80** 3777
Boehler R 1986 *Geophys. Res. Lett.* **13** 1153
[3] Anderson O L 1986 *Geophys. R. Astron. Soc.* **84** 561
[4] Hafner J 1987 *Springer Series in Solid State Sciences* vol 70 (Heidelberg: Springer)
[5] Stroud D and Ashcroft N W 1972 *Phys. Rev.* B **5** 371
[6] Jones H D 1973 *Phys. Rev.* A **8** 3215
[7] Pélissier J L 1984 *Physica* A **126** 474
[8] Young D A and Ross M 1984 *Phys. Rev.* B **29** 682
[9] Pélissier J L 1984 *Physica* A **128** 363
[10] Moriarty J A, Young D A and Ross M 1984 *Phys. Rev.* B **30** 578
[11] Pélissier J L 1984 *Phys. Lett.* **103A** 345
[12] Pélissier J L 1984 *Physica* A **126** 271
[13] Holian B L, Straub G K, Swanson R E and Wallace D C 1983 *Phys. Rev.*B **27** 2873
[14] Walker A B, Smith W and Inglesfield J E 1986 *J. Phys. F: Met. Phys.* **16** L35
[15] Broughton J Q and Li X P 1987 *Phys. Rev.* B **35** 9120
[16] Igloi F, Kahl G and Hafner J 1987 *J. Phys. C: Solid State Phys.* **20** 1803

[17] Wills J M and Harrison W A 1983 *Phys. Rev.* B **28** 4363
[18] Hausleitner C and Hafner J 1988 *J. Phys. F: Met. Phys.* **18** 1025
[19] Williams A R, Moruzzi V and Janak J F 1978 *Calculated Electronic Properties of the Elements* (New York: Pergamon)
[20] Harrison W A and Froyen S 1980 *Phys. Rev.* B **21** 3214
[21] Isihara A 1968 *J. Phys. A: Math. Gen.* **1** 29
[22] Leung C H, Stott M J and Young W M 1976 *J. Phys. F: Met. Phys.* **6** 1039
[23] Waisman E 1973 *Mol. Phys.* **25** 45
[24] Grimvall G 1975 *Phys. Scr.* **12** 173; 1976 *Phys. Scr.* **13** 59
[25] Madsen J, Andersen O K, Poulsen U K and Jepsen O 1976 *AIP Conf. Proc.* **29** 327
[26] Hasegawa H and Pettifor D G 1983 *Phys. Rev. Lett.* **50** 130
[27] Grimvall G 1974 *Solid State Commun.* **14** 551
[28] Gschneider K A 1964 *Solid State Phys.* **16** 313ff (New York: Academic)
[29] Hultgren R, Orr R L, Anderson P D and Kelley K K 1973 *Selected Values of Thermodynamic Properties of Metals and Alloys* (New York: Wiley)
[30] Smithells C J and Brandes W L (ed.) 1983 *Metal Reference Book* 6th edn (London: Butterworth)
[31] Shimoji M 1977 *Liquid Metals* (New York: Academic)
[32] Lindemann F A 1910 *Z. Phys.* **11** 609
[33] Verlet L 1968 *Phys. Rev.* **165** 201
[34] Hansen J P and Verlet L 1969 *Phys. Rev.* **184** 150